

## Uptake of reactive nitrogen on cirrus cloud particles during INCA

H. Ziereis,<sup>1</sup> A. Minikin,<sup>1</sup> H. Schlager,<sup>1</sup> J. F. Gayet,<sup>2</sup> F. Auriol,<sup>3</sup> P. Stock,<sup>1</sup> J. Baehr,<sup>1</sup>  
A. Petzold,<sup>1</sup> U. Schumann,<sup>1</sup> A. Weinheimer,<sup>4</sup> B. Ridley,<sup>4</sup> and J. Ström<sup>5</sup>

Received 8 October 2003; revised 18 December 2003; accepted 12 February 2004; published 11 March 2004.

[1] The uptake of reactive nitrogen species on ice crystals in cirrus clouds was investigated by simultaneous aircraft-based measurements of gas- and condensed-phase  $\text{NO}_y$ , ice particle size distribution and total aerosol surface area. The measurements were performed in 2000 during the INCA campaign at northern and southern midlatitudes at local autumn. Cirrus ice particles were frequently encountered during these flights in the upper troposphere. Concurrently with the occurrence of cirrus ice particles particulate  $\text{NO}_y$  was observed. It was found that the coverage of the cirrus ice particles with particulate  $\text{NO}_y$  strongly depends on the temperature and the gas-phase  $\text{NO}_y$  concentration. A substantial coverage of the ice particles with values larger than one percent of a monolayer was observed only for temperatures below about 217 K. On average only about one percent of the available gas-phase  $\text{NO}_y$  was found as particulate  $\text{NO}_y$ . **INDEX TERMS:** 0305 Atmospheric Composition and Structure: Aerosols and particles (0345, 4801); 0320 Atmospheric Composition and Structure: Cloud physics and chemistry; 0365 Atmospheric Composition and Structure: Troposphere—composition and chemistry. **Citation:** Ziereis, H., et al. (2004), Uptake of reactive nitrogen on cirrus cloud particles during INCA, *Geophys. Res. Lett.*, 31, L05115, doi:10.1029/2003GL018794.

### 1. Introduction

[2] Laboratory experiments and model investigations have studied the uptake of gas-phase  $\text{HNO}_3$  by water-ice films [Abbatt, 1997; Zondlo et al., 1997; Tabazadeh et al., 1999; Hudson et al., 2002; Hynes et al., 2002]. These studies suggest that cirrus clouds have the potential to lead to a substantial removal of  $\text{HNO}_3$  from the gas-phase. A considerable reduction of  $\text{HNO}_3$  throughout the upper troposphere caused by gravitational settling of  $\text{HNO}_3$  covered ice particles was simulated by Lawrence and Crutzen [1998]. Investigations with a chemical box model studied the impact of this redistribution on the chemistry of the midlatitude upper troposphere [Meier and Hendricks, 2002]. These simulations suggest that cirrus cloud chemistry has the potential to induce reductions in ozone by up to 14% in some regions of the upper troposphere.

<sup>1</sup>Deutsches Zentrum für Luft- und Raumfahrt (DLR), Oberpfaffenhofen, Germany.

<sup>2</sup>Laboratoire de Météorologie Physique, Université Blaise Pascal, Aubière, France.

<sup>3</sup>Laboratoire d'Optique Atmosphérique, Université des Sciences et Technologies de Lille, Villeneuve, France.

<sup>4</sup>NCAR, Boulder, Colorado, USA.

<sup>5</sup>Institute of Applied Environmental Research (Air Pollution Laboratory), Stockholm University, Stockholm, Sweden.

[3] In recent years some in-situ investigations of the uptake of gas-phase  $\text{HNO}_3$  on the surface of cirrus cloud particles in the upper troposphere have been performed [Weinheimer et al., 1998; Feigl et al., 1999; Schlager et al., 2001; Kondo et al., 2003]. However, the number of these observations is still too small to develop a consistent perception of the atmospheric importance of this process. Furthermore, most of these measurements were performed at temperatures below about 215 K.

[4] This paper reports observations of particulate nitrate made during the INCA (Interhemispheric differences in cirrus properties from anthropogenic emissions) experiment in 2000. Aircraft measurements were performed in March/April and September/October, respectively, out of Punta Arenas (Chile) and Prestwick (Scotland). Particulate nitrate, gas-phase  $\text{NO}_y$  along with other trace gases and different aerosol parameters were measured during 14 flights. These data are compared to the results of previous aircraft measurements and model simulations.

### 2. Measurements

[5] The experimental approach chosen to measure particulate nitrate during INCA is quite similar to that used during previous measurements [Weinheimer et al., 1998; Feigl et al., 1999; Kondo et al., 2003]. Gas-phase total reactive nitrogen,  $\text{NO}_y$ , and particulate nitrate were measured by employing forward- and aft-facing inlets with separate detection channels. The inlets were made of 3/8-inch outer diameter Teflon tubes heated to about 30°C. The aft-facing inlet discriminates against the collection of cloud ice particles and therefore provides measurements that are dominated by gas-phase  $\text{NO}_y$ . The forward-facing inlet is subsokinetic and samples particles with an enhanced efficiency relative to the gas-phase. Condensed-phase  $\text{NO}_y$  ( $\text{PNO}_y$ ) expressed as gas-phase equivalent is inferred from the difference between forward- and aft-facing inlet  $\text{NO}_y$  signals corrected by the effective enhancement factor (EF). EF is determined by the Stokes number of the sampled particles, the true air speed of the aircraft and the sample flow into the inlet. For particles with diameter larger than 15–20  $\mu\text{m}$  EF is very close to its upper limit and does not depend on the size of the sampled particles. Particles containing  $\text{NO}_y$  are completely evaporated and measured as gas-phase  $\text{NO}_y$  using the conventional  $\text{NO}_y$  – converter technique and NO chemiluminescence. Outside cirrus clouds the  $\text{NO}_y$  signals of the two channels agreed within 15 pptv. The limit for the detection of  $\text{PNO}_y$  was consequently determined by dividing this number by EF yielding a value of about 0.1 pptv.

[6] During previous observations, the high mass limit EF of the respective instrument was chosen to calculate  $\text{PNO}_y$ . For this study, however, the size dependent EF was calcu-

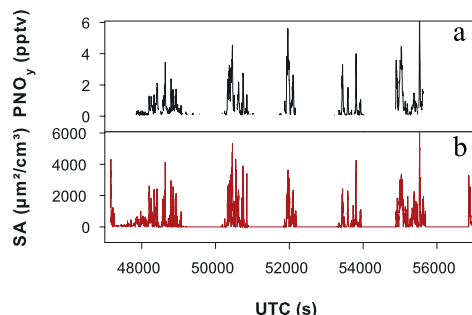


**Figure 1.** (a) Particle  $\text{NO}_y$  as gas-phase equivalent in pptv and (b) SA in  $\mu\text{m}^2/\text{cm}^3$  for the flight on April 12, 2000.

lated from the measured particle size distribution. For some cases this value differed significantly from the maximum EF. The sampling efficiency of the inlet was calculated by using an empirically derived function. This function was determined by wind tunnel measurements in our laboratory for small Stokes numbers and confirmed by a computational fluid dynamics model [Krämer and Afchine, 2004]. The mean enhancement factor for all flights was 110 with a standard deviation of 29. For typical flight conditions at 323 hPa and 228 K the derived enhancement factor was 109 for a particle diameter of 30  $\mu\text{m}$  and 69 for a diameter of 12  $\mu\text{m}$  while the maximum enhancement factor would have been 119.

[7] The particle size distribution was determined with a PMS FSSP-300 operated by DLR and a PMS 2D-C operated by LaMP. The combination of these two techniques provides the particle size distribution between 3 and 800  $\mu\text{m}$  [Gayet et al., 2002a]. During previous atmospheric measurements the surface area density (SA) was derived from particle size distributions and total water measurements. During INCA the SA was measured by means of a polar nephelometer (PN) operated by LaMP [Gayet et al., 2002b]. The PN measures the scattering phase function and extinction coefficient of an ensemble of cloud particles between a few micrometers to about 800  $\mu\text{m}$ . SA is subsequently derived from the extinction coefficient.

[8] In our analysis we have to assume that  $\text{HNO}_3$  is the main or only component of  $\text{NO}_y$  that is adsorbed on ice surfaces because  $\text{HNO}_3$  was not measured separately. For the following considerations a  $\text{HNO}_3/\text{NO}_y$  ratio of 0.5 was assumed.

[9] The measurement uncertainty of  $\text{PNO}_y$  depends on the accuracy of the  $\text{NO}_y$  measurements and on the accuracy of the EF determination. The uncertainty of EF is mainly controlled by the uncertainty of the measurement of the particle size distribution. Assuming typical uncertainties for the particle size determination [Gayet et al., 2002a] the combined error for a  $\text{PNO}_y$  concentration of 1 pptv is 28% for 30  $\mu\text{m}$  particles and 53% for 12  $\mu\text{m}$  particles. The uncertainty of the coverage also depends on SA. With an uncertainty of 25% for the determination of SA [Gayet et al., 2002b] the overall uncertainty of the coverage is about 58% for 12  $\mu\text{m}$  particles and 38% for 30  $\mu\text{m}$  particles. For almost all cases the overall uncertainty of the coverage is

smaller than the standard deviation of the measurements at a given temperature.

### 3. Results and Discussion

[10] Most cirrus observations during INCA were made at around 9000 m altitude. Cirrus properties were often highly variable. In situ water vapor measurements found that the humidity with respect to ice (RHI) showed a large variability inside the cirrus clouds [Ovarlez et al., 2002]. Observed cirrus ice surface area densities (SA) varied over a wide range with maximum values of more than 28000  $\mu\text{m}^2/\text{cm}^3$ . Median values of the SA at Punta Arenas and Prestwick were 243 and 356  $\mu\text{m}^2/\text{cm}^3$ , respectively. Enhanced condensed phase  $\text{NO}_y$  ( $\text{PNO}_y$ ) was observed at temperatures between 212 and 248 K. Temperatures below about 217 K were only encountered during the southern-hemisphere experiment.  $\text{PNO}_y$  was observed during all flights in connection with the occurrence of cirrus cloud elements as reflected by the increase in SA. As an example, results for the flight on April 12, 2000 out of Punta Arenas are presented in Figure 1. During this flight a cirrus cloud was probed several times at an altitude between 9 and 10 km.  $\text{PNO}_y$  and SA are shown as a time series.

[11] Observed  $\text{PNO}_y$  inside clouds ( $\text{SA} > 10 \mu\text{m}^2/\text{cm}^3$ ) was highly variable with values ranging between the detection limit and about 80 pptv. The median values for the southern and northern hemisphere in cloud measurements were 0.4 pptv and 1.2 pptv, respectively. As the observed  $\text{PNO}_y$  depends on the available ice SA, the coverage is a more suitable parameter to describe the uptake of  $\text{HNO}_3$  on surfaces. Furthermore it facilitates the comparison with model calculations and previous observations. The coverage is defined as the number of molecules adsorbed on the surface of the cirrus ice elements per site available in a monolayer on a unit surface area. A monolayer is assumed to comprise  $10^{15}$  molecules per  $\text{cm}^2$  ice surface.

[12] Models of the uptake of  $\text{HNO}_3$  on ice surfaces suggest that the coverage depends on temperature and on the nitric acid partial pressure ( $p\text{-HNO}_3$ ) [e.g., Tabazadeh et al., 1999]. In Figure 2 the deduced coverage expressed as a fraction of a monolayer is shown versus temperature for SA larger than  $10 \mu\text{m}^2/\text{cm}^3$  for all 14 flights. Additionally to the 1-s data, values averaged over temperature intervals of 1 K are shown along with its standard deviations. The highest average coverages up to 0.15 were observed for temper-

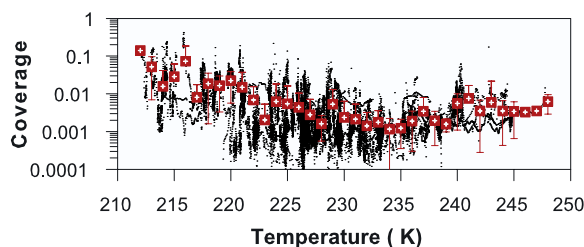


**Figure 2.** Observed coverages during INCA (in  $10^{15}$  molecules/ $\text{cm}^2$ ) versus temperature for all flights and  $\text{SA} > 10 \mu\text{m}^2/\text{cm}^3$ . 1-s values along with means and standard deviations. The values have been averaged over temperature intervals of 1 degree.

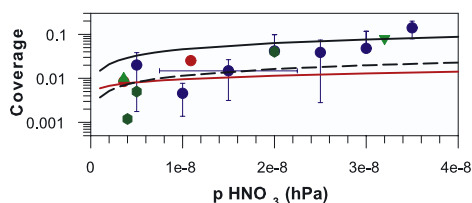


**Figure 3.** Observed coverages averaged over  $p\text{-HNO}_3$  intervals of  $0.5 \times 10^{-8}$  hPa along with standard deviations versus  $p\text{-HNO}_3$  for temperatures below 217 K. An error bar assuming an uncertainty of 50% for our estimated  $\text{HNO}_3/\text{NO}_y$  ratio is added to one data point. For comparison, calculated coverages and coverages measured during previous aircraft campaigns are shown. Measurements: Red circle (SUCESS: [Weinheimer et al., 1998]), green triangles (POLSTAR1/2: [Feigl et al., 1999; Schlager et al., 2001]), dark green diamonds (BIBLE/SOLVE: [Kondo et al., 2003]), blue circles: (INCA). Model calculations: Black line and black dashed line [Tabazadeh et al., 1999] for a binding energy of  $-14.2$  and  $-13$  kcal/mol, respectively, red line [Hudson et al., 2002]. Coverages have been calculated for the median temperature of this sub data set (214 K).

atures below about 217 K. The observed coverages decrease substantially with increasing temperature.

[13] The two INCA field campaigns were performed in regions with substantial differences in trace gas concentration [Baehr et al., 2003]. Median  $\text{NO}_y$  volume mixing ratios observed in the upper troposphere were 76 pptv at southern and 225 pptv at northern midlatitudes, respectively. This difference is also reflected in the observed coverages with median values of 0.14% and 0.36%, respectively, for temperatures above 217 K. Although higher coverages and surface areas were found in the north, the ratio between particulate nitrate and gas-phase  $\text{NO}_y$  was higher in the south, 0.7% compared to 0.5%. This is caused by the lower gas-phase  $\text{NO}_y$  volume mixing ratios found there.

[14] Most of the previous atmospheric measurements of  $\text{PNO}_y$  were made at temperatures between about 196 and 215 K. In Figure 3 coverages observed for temperatures below 217 K are compared to the results of previous measurements. The observed coverages have been averaged over  $p\text{-HNO}_3$  intervals of  $0.5 \times 10^{-8}$  hPa. The coverages observed increase with increasing  $p\text{-HNO}_3$  as predicted by models. Measurements at higher temperatures were reported only by Kondo et al. [2003]. For  $p\text{-HNO}_3$  of about  $0.5 \times 10^{-8}$  hPa and temperatures between about 210 and 250 K coverages of 0.001 to 0.005 of a monolayer were observed during the BIBLE aircraft program over the tropical Pacific Ocean. In general, the present data agrees reasonably well with the results of the previous experiments within the uncertainty range of the INCA measurements.

[15] In Figure 4 coverages obtained during INCA are presented versus  $p\text{-HNO}_3$ . The data were confined to the range between the 25 and 75 percentile around the median in cloud temperature observed during INCA (226.8 K). 1-s values are given along with values averaged over  $p\text{-HNO}_3$  intervals of  $1 \times 10^{-8}$  hPa. Although the observed coverages show a substantial scatter a clear increase of the coverage with

$p\text{-HNO}_3$  was found. For comparison, values calculated with the Frenkel-Halsey-Hill (FHH) model of Hudson et al. [2002] and with the adsorption model of Tabazadeh et al. [1999] are presented. These values have been calculated for the median temperature of this data set and have been normalized to a monolayer of  $10^{15}$  molecules/cm<sup>2</sup> ice surface. Based on laboratory investigations Tabazadeh et al. [1999] derived a binding energy for  $\text{HNO}_3$  adsorbed on ice of  $-14.2$  kcal/mol. However, a better agreement between this adsorption model and the present data at this temperature range was achieved by assuming a binding energy of  $-12$  kcal/mol. The values calculated with the FHH – model overestimate the measured coverages especially for low  $p\text{-HNO}_3$ . In the low temperature regime (see Figure 3) most of the observed coverages are between the Tabazadeh model curves for binding energies of  $-14$  and  $13$  kcal/mol. In this temperature region the FHH model underestimates most of the observed values.

[16] A considerable uncertainty arises from the lack of  $\text{HNO}_3$  measurements during INCA. However, even a much lower  $\text{HNO}_3/\text{NO}_y$  ratio than 0.5 as assumed for this analysis would not reconcile the present observations with model predictions for temperatures higher than about 217 K (see uncertainty bar in Figure 4). The low coverages and their high variation observed during INCA suggest that temperature and partial pressure are not the only parameters controlling the uptake of  $\text{HNO}_3$  on ice. Although, both models and observations show some agreement in the dependence of the uptake on temperature and  $p\text{-HNO}_3$ , the deviations between observed and calculated coverages at least for higher temperatures are substantial. This discrepancy might be caused by the following reasons: The model simulations based on laboratory measurements might not be appropriate to describe real cirrus clouds and the uptake of  $\text{HNO}_3$  on it. The uptake of  $\text{HNO}_3$  on cirrus cloud elements might be limited by its lifetime with respect to heterogeneous loss. For a temperature of 226.8 K and a SA of  $300 \mu\text{m}^2/\text{cm}^3$ , the temperature dependent uptake coefficients given by Hudson et al. [2002] and Hynes et al. [2002] lead to lifetimes of about 10.6 hours and 1.4 hours,

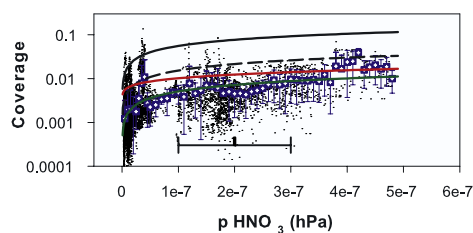


**Figure 4.** Observed coverages averaged over  $p\text{-HNO}_3$  intervals of  $1.0 \times 10^{-8}$  hPa versus  $p\text{-HNO}_3$  for temperatures within the 25 and 75 percentile around the median value of 226.8 K. Model calculated values: Tabazadeh et al. [1999] for binding energies of  $-14.2$  kcal/mol (black line),  $-13$  kcal/mol (black dashed line), and  $-12$  kcal/mol (green line); Hudson et al. [2002]: red line. Coverages have been calculated for 226.8 K. An error bar of 50% for our assumed  $\text{HNO}_3/\text{NO}_y$  ratio is added to one data point ( $p\text{-HNO}_3 = 2 \times 10^{-7}$  hPa) below the respective value at the bottom of this figure.

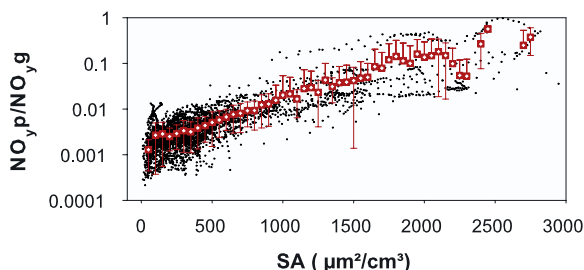


**Figure 5.** PNO<sub>y</sub>/NO<sub>y,gas</sub> SA. The ratios are plotted for temperatures and partial pressures within the 25 and 75 percentiles around the respective median values of 226.8 K and  $1.37 \cdot 10^{-8}$  hPa, respectively. The 1-s data of the ratio are given along with means and standard deviations. The 1-s values have been averaged over SA intervals of  $50 \mu\text{m}^2/\text{cm}^3$ .

respectively. However, a lifetime of only 4 min arises assuming the temperature independent uptake coefficient given by Abbott [1997]. Furthermore, the assumption that the cirrus ice particles are in equilibrium might not be valid considering the substantial range of the relative humidity with respect to ice inside cirrus clouds as observed during INCA [Ovarlez et al., 2002] indicating that a large fraction of the encountered clouds were in the formation or dissipation phase.

[17] In Figure 5 the PNO<sub>y</sub>/NO<sub>y</sub> ratio is shown versus SA. The data range for this analysis has been confined to temperatures and partial pressures within the 25 and 75 percentiles around the respective median values of 226.8 K and  $1.37 \cdot 10^{-8}$  hPa. A clear dependence of this ratio on the SA was found. The highest values were obtained during a flight on April 13. Although the coverage was only about 1%, for this particular case the combination of low gas-phase NO<sub>y</sub> (40 pptv) and high SA ( $2000 \mu\text{m}^2/\text{cm}^3$ ) led to a ratio between condensed-phase and gas-phase NO<sub>y</sub> of about 1.

[18] In general only a small fraction of the total available NO<sub>y</sub> was found as particulate nitrate for the conditions encountered during INCA. Therefore, a substantial depletion of the gas-phase HNO<sub>3</sub> can not be expected and the effect on the atmospheric chemistry should be small. However, the general atmospheric implications of these findings are difficult to assess. The HNO<sub>3</sub> uptake was found to depend sensitively on temperature, p-HNO<sub>3</sub>, and SA. According to SAGE measurements, typical cirrus clouds are found at altitudes of 70% to 80% of the local tropopause height [Dowling and Radke, 1990]. In this altitude region temperatures are in general above 220 K. Therefore, for median coverages and SA as observed during INCA, the depletion of HNO<sub>3</sub> by uptake on cirrus cloud particles is not expected to lead to a major perturbation of the ozone chemistry of the upper troposphere at midlatitudes in spring and fall. However, this does not exclude a substantial depletion of gas-phase HNO<sub>3</sub> for individual cases. Furthermore, for other regions of the atmosphere, like the colder tropical tropopause region, and for other seasons, the conditions might be more favorable for a significant uptake of HNO<sub>3</sub> on ice particles.

[19] **Acknowledgments.** We would like to thank the DLR Flight Department for the expert support during the INCA campaigns. We are grateful to M. Krämer, J. Hendricks, P. Popp and B. Kärcher for very helpful discussions. This research has been funded in part by the Commission of the European Community under contract EVK2-CT-1999-00039.

## References

- Abbott, J. P. D. (1997), Interaction of HNO<sub>3</sub> with water-ice surfaces at temperatures of the free troposphere, *Geophys. Res. Lett.*, *24*, 1479–1482.
- Baehr, J., H. Schlager, H. Ziereis, P. Stock, P. van Velthoven, R. Busen, J. Ström, and U. Schumann (2003), Aircraft observations of NO, NO<sub>y</sub>, CO, and O<sub>3</sub> in the upper troposphere from 60°N to 60°S — Interhemispheric differences at midlatitudes, *Geophys. Res. Lett.*, *30*(11), 1598, doi:10.1029/2003GL016935.
- Dowling, D. R., and L. F. Radke (1990), A summary of the physical properties of cirrus clouds, *J. Appl. Meteorol.*, *29*, 970–978.
- Feigl, C., H. Schlager, H. Ziereis, J. Curtius, F. Arnold, and C. Schiller (1999), Observation of NO<sub>y</sub> uptake by particles in the Arctic tropopause region at low temperatures, *Geophys. Res. Lett.*, *26*, 2215–2218.
- Gayet, J.-F., F. Auriol, A. Minikin, J. Ström, M. Seifert, R. Krejci, A. Petzold, G. Febvre, and U. Schumann (2002a), Quantitative measurement of the microphysical and optical properties of cirrus clouds with four different in situ probes: Evidence of small ice crystals, *Geophys. Res. Lett.*, *29*(24), 2230, doi:10.1029/2001GL014342.
- Gayet, J.-F., S. Asano, A. Yamazaki, A. Uchiyama, A. Sinyuk, O. Jourdan, and F. Auriol (2002b), Two case studies of continental-type water and maritime mixed-phased stratocumuli over the sea: 1. Microphysical and optical properties, *J. Geophys. Res.*, *107*(D21), 4569, doi:10.1029/2001JD001106.
- Hudson, P. K., et al. (2002), Uptake of HNO<sub>3</sub> on ice at tropospheric temperatures: Implications for cirrus clouds, *J. Phys. Chem. A*, *106*, 9874–9882.
- Hynes, R. G., M. A. Fernandez, and R. A. Cox (2002), Uptake of HNO<sub>3</sub> on water-ice and coadsorption of HNO<sub>3</sub> and HCl in the temperature range 210–235 K, *J. Geophys. Res.*, *107*(D24), 4797, doi:10.1029/2001JD001557.
- Kondo, Y., et al. (2003), Uptake of reactive nitrogen on cirrus cloud particles in the upper troposphere and lowermost stratosphere, *Geophys. Res. Lett.*, *30*(4), 1154, doi:10.1029/2002GL016539.
- Krämer, M., and A. Afchine (2004), Sampling characteristics of inlets operated at low U/U<sub>0</sub> ratios: New insights from computational fluid dynamics (CFX) modeling, *J. Aerosol Sci.*, in press.
- Lawrence, M. G., and P. J. Crutzen (1998), The impact of cloud particle gravitational settling on soluble trace gas distributions, *Tellus, Ser. B*, *50*, 263–289.
- Meier, A., and J. Hendricks (2002), Model studies on the sensitivity of upper tropospheric chemistry to heterogeneous uptake of HNO<sub>3</sub> on cirrus ice particles, *J. Geophys. Res.*, *107*(D23), 4696, doi:10.1029/2001JD001735.
- Ovarlez, J., J. Gayet, K. Gierens, J. Ström, H. Ovarlez, F. Auriol, R. Busen, and U. Schumann (2002), Water vapour measurements inside cirrus clouds in Northern and Southern hemispheres during INCA, *Geophys. Res. Lett.*, *29*(16), 1813, doi:10.1029/2001GL014440.
- Schlager, H., et al. (2001), In situ observations of particulate NO<sub>y</sub> in cirrus clouds for different atmospheric conditions, *Proceedings of the European Workshop: Aviation, Aerosols, Contrails and Cirrus Clouds (A2C3)*, Seeheim, Germany, July 10–12, 2000, edited by U. Schumann and G. T. Amanatides, pp. 68–73, Eur. Comm., Brussels.
- Tabazadeh, A., O. B. Toon, and E. J. Jensen (1999), A surface chemistry model for nonreactive trace gas adsorption on ice: Implications for nitric acid scavenging by cirrus, *Geophys. Res. Lett.*, *26*, 2211–2214.
- Weinheimer, A. J., T. L. Campos, J. G. Walega, F. E. Grahek, B. A. Ridley, D. Baumgardner, C. H. Twohy, and B. Gandrud (1998), Uptake of NO<sub>y</sub> on wave-cloud ice particles, *Geophys. Res. Lett.*, *25*, 1725–1728.
- Zondlo, M. A., S. B. Barone, and M. A. Tolbert (1997), Uptake of HNO<sub>3</sub> on ice under upper tropospheric conditions, *Geophys. Res. Lett.*, *24*, 1391–1394.
- F. Auriol, Laboratoire d'Optique Atmosphérique, Université des Sciences et Technologies de Lille, Villeneuve, France.
- J. Baehr, A. Minikin, A. Petzold, H. Schlager, U. Schumann, P. Stock, and H. Ziereis, DLR, Institute for Atmospheric Physics, Oberpfaffenhofen, Wessling, D-82230, Germany. (helmut.ziereis@dlr.de)
- J. F. Gayet, Laboratoire de Météorologie Physique, Université Blaise Pascal, Aubière, France.
- B. Ridley and A. Weinheimer, NCAR, Boulder, Colorado, USA.
- J. Ström, Institute of Applied Environmental Research (Air Pollution Laboratory), Stockholm University, Stockholm, Sweden.